MOLECULAR AND CELLULAR BIOLOGY, Jan. 2005, p. 699–705 Vol. 25, No. 2
0270-7306/05/$08.00+0 doi:10.1128/MCB.25.2.699–705.2005

Tenomodulin Is Necessary for Tenocyte Proliferation and Tendon Maturation

Denitsa Docheva,[1] Ernst B. Hunziker,[2] Reinhard Fässler,[1]* and Oliver Brandau[1]†

Department of Molecular Medicine, Max Planck Institute for Biochemistry, Martinsried, Germany,[1] and ITI Research Institute, University of Berne, Berne, Switzerland[2]

Received 15 October 2004/Accepted 26 October 2004

Tenomodulin (Tnmd) is a member of a new family of type II transmembrane glycoproteins. It is predominantly expressed in tendons, ligaments, and eyes, whereas the only other family member, chondromodulin I (ChM-I), is highly expressed in cartilage and at lower levels in the eye and thymus. The C-terminal extracellular domains of both proteins were shown to modulate endothelial-cell proliferation and tube formation in vitro and in vivo. We analyzed Tnmd function in vivo and provide evidence that Tnmd is processed in vivo and that the proteolytically cleaved C-terminal domain can be found in tendon extracts. Loss of Tnmd expression in gene targeted mice abated tenocyte proliferation and led to a reduced tenocyte density. The deposited amounts of extracellular matrix proteins, including collagen types I, II, III, and VI and decorin, lumican, aggrecan, and matrilin-2, were not affected, but the calibers of collagen fibrils varied significantly and exhibited increased maximal diameters. Tnmd-deficient mice did not have changes in tendon vessel density, and mice lacking both Tnmd and ChM-I had normal retinal vascularization and neovascularization after oxygen-induced retinopathy. These results suggest that Tnmd is a regulator of tenocyte proliferation and is involved in collagen fibril maturation but do not confirm an in vivo involvement of Tnmd in angiogenesis.

Tendons and ligaments connect the elements of the musculoskeletal system and are composed of a densely packed collagen-rich connective tissue able to withstand high tensile forces. Collagen type I is predominant, but collagen types III, IV, V, and VI, and proteoglycans are also deposited into the tendon extracellular matrix (ECM) (5, 28). Proteoglycans are important for spacing and lubrication of tendon fibrils and regulate lateral collagen fibril growth (13, 17, 18, 44, 47). The cellular content of tendons is dominated by tenocytes, which are arranged in longitudinal rows. Tenocytes have sheet-like extensions, which surround the collagen fibrils and create cell-cell and cell-ECM interactions (30, 41). Vascularization of tendons is sparse, and endothelial cells and other cell types such as mast cells and cells of the peripheral nervous system are rare and mainly found in the connective tissue sheets which surround the tendon fascicles (5). A protein, which was suggested to play a role in tendon development and vascularization is Tenomodulin (Tnmd, Tendin, CHM1L, TeM, and Myodulin), a recently identified member of a new family of type II transmembrane proteins (12, 45, 50). It is predominantly expressed in tendons, ligaments, and the eye (12, 45, 50), but low levels of m-RNA transcripts have also been identified in muscle, thymus, heart, liver, spleen, nervous tissues, lungs, and cartilage (12). The only close homologue chondromodulin I (ChM-I) is highly expressed in cartilage and to a lower extent in eye and thymus (12, 23, 26, 34), leading to both distinct and overlapping expression patterns of Tnmd and ChM-I. The extracellular part of both proteins contains two extracellular domains: BRICHOS and a C-terminal cysteine-rich domain, the latter of which is exclusively found in ChM-I and Tnmd. The BRICHOS domain was first identified in BRI (for British dementia), ChM-I, and SP-C (for surfactant-associated protein C) (43). It consists of a conserved sequence of approximately 100 amino acids adjacent to proteolytic cleavage sites, but its function remains unclear (43). Proteolytic cleavage of ChM-I by furin occurs at the C-terminal of the BRICHOS domain and leads to the secretion of the C-terminal cysteine-rich domain into the ECM. The remaining membrane bound part has a short half-life and can apparently not be detected in tissue samples (3). Processing of Tnmd has not been experimentally analyzed, but a putative protease recognition sequence RXXR was identified (4). Similar to ChM-I, cleavage at this site would release the C-terminal cysteine-rich domain of Tnmd from the cell membrane (12).

The secreted C-terminal cysteine-rich domains of ChM-I and Tnmd act as regulators of cell proliferation and differentiation. The recombinant C-terminal cysteine-rich domain of ChM-I increased proliferation of primary chondrocytes (26, 27), whereas endothelial proliferation and tube formation were inhibited by the ectopic endothelial expression of the C-terminal cysteine-rich domain of either Tnmd or ChM-I (36, 37). Expression of the full-length Tnmd in endothelial cells increased their proliferation (37), and endothelial proliferation was also enhanced by expression of the full-length Tnmd on cocultured myoblasts (40). In vivo, human melanoma cells transduced with the secretable C-terminal cysteine-rich domains of Tnmd or ChM-I showed decreased tumor growth and vascularization (37). However, deletion of ChM-I in mice did not affect endothelial or chondrocyte proliferation. Since the Tnmd gene was not upregulated in ChM-I-deficient tissue, the lack of ChM-I is likely to be compensated by other factors (11).

To investigate the role of Tnmd in vivo, we generated Tnmd-

* Corresponding author. Mailing address: Max Planck Institute for Biochemistry, Department of Molecular Medicine, Am Klopferspitz 18, 82152 Martinsried, Germany. Phone: 49-89-8578-2424. Fax: 49-89-8578-2422. E-mail: faessler@biochem.mpg.de.

† Present address: Department of Physiology, LMU-München, 80336 Munich, Germany.

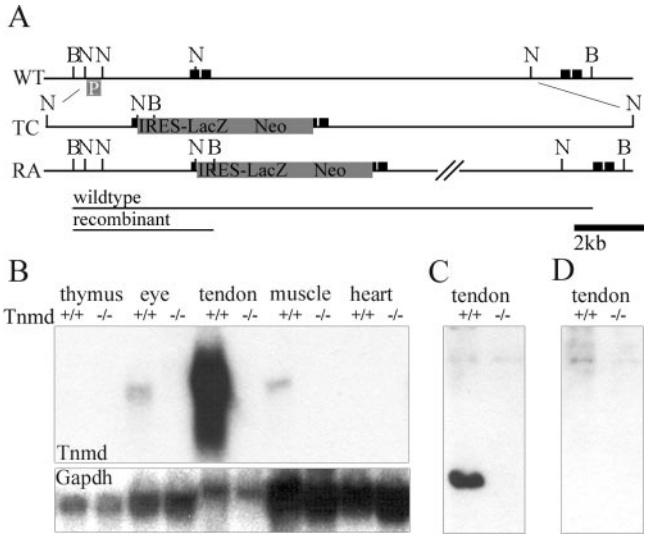

FIG. 1. Generation of Tnmd-deficient mice. (A) An IRES-LacZ neomycin cassette was inserted into the translation start site in exon 1 of the Tnmd gene. (B) Hybridization of total RNA derived from newborn thymus, eye, tendon, muscle and heart tissues with the complete Tnmd cDNA showed the lack of any Tnmd transcript (1.4 kb) in the *Tnmd* gene-targeted mice. (C) A specific signal for Tnmd was detected at 16 kDa in urea tendon extracts of 1-month-old mice. (D) No signal was found in extracts from Tnmd-deficient mice or after incubation with the peptide, used for immunization. B, BamHI; N, NcoI; p, southern probe; black boxes, exons; WT, wild-type allele; TC, targeting construct; RA, recombinant allele.

deficient mice. We observed reduced cell numbers in adult tendons and a decrease in tenocyte proliferation at newborn stage. In addition, the altered structure of adult collagen fibrils suggests an involvement of Tnmd in postnatal tendon maturation. Angiogenesis was unchanged in tendons. The controversial in vitro and in vivo studies regarding the role of ChM-I and Tnmd for angiogenesis led us to investigate retinal neovascularization, which was unaffected after oxygen-induced retinopathy (OIR) in mice lacking both Tnmd and ChM-I.

MATERIALS AND METHODS

Generation of Tnmd-deficient mice. The complete cDNA of Tnmd (12) was used to hybridize a 129/sv mouse phage 1 P1-derived artificial chromosome (PAC) library (RPCI21) (38). Two NcoI fragments of 2.3 and 8 kb were subcloned from PAC 354-K9, sequenced to establish the exon-intron boundaries of exon 1, and subsequently inserted into a vector consisting of an internal ribosomal entry site (IRES), a LacZ reporter gene, and a neomycin-resistant cassette with PGK promoter and poly(A) signal sequences, respectively (Fig. 1A). The targeting construct was electroporated into passage 11 R1 embryonic stem (ES) cells. After G418 selection, 360 ES cell clones were isolated and screened for homologous recombination by probing BamHI-digested DNA with a 600-bp external NcoI fragment (Fig. 1A). Targeted ES cells were injected into blastocysts to generate germ line chimeras, which were subsequently mated with C57BL/6 females. Genotyping was performed either by Southern blotting as described above or by PCR by using forward primers in the 5′-untranslated region (AACTCCACCTCAGCAGTAGTCC) of the *Tnmd* gene and the PGK poly(A) signal sequence of the neomycin cassette (GATTAGATAAATGCCT GCTC) and a reverse primer in exon 2 (TTCTTGGATACCTCGGGCCAG).

Northern blot analysis. Tissue RNA was isolated from newborn and 1-month-old mice by using TRIzol reagent in accordance to the manufacturer's instructions (Invitrogen). For Northern analysis, 10 μg of total RNA was size fractionated on a 1% agarose–2.2 M formaldehyde gel, transferred to a Hybond-XL membrane (Amersham), and hybridized with a ^{32}P-labeled cDNA probe specific for the entire Tnmd coding sequence (nucleotides 1 to 740).

Skeletal analysis. For whole-mount skeletal staining, newborn and 6-week-old Tnmd-deficient and control mice were sacrificed by CO_2 inhalation. Skeletons were dissected and stained with Alcian blue and Alizarin red as previously described (2). For X-ray imaging analysis, 6-month-old Tnmd-null and control mice were sacrificed, dissected, and fixed in 70% ethanol. X-ray images were obtained with a Siemens Polymat 70 at 48 kV and 0.2 mA.

Histology and immunohistochemistry. For histological analysis, tissues dissected at embryonic and adult stages were fixed overnight in fresh 4% paraformaldehyde (PFA) in phosphate-buffered saline (PBS; pH 7.4) or in 95% ethanol–5% glacial acetic acid. Samples from mice older than 3 days were decalcified in 10% EDTA–1× PBS for 5 days. After paraffin or cryomatrix embedding, sections were cut at 6 and 10 μm, respectively.

Hematoxylin and eosin (HE) staining, toluidine blue staining, and immunostainings for collagens α2(I), α1(II), α1(III), α1(VI), α2(VI), α3(VI), decorin, aggrecan, lumican, matrilin-2, and endomucin were performed as previously described (2, 19, 47). For antibody detection Cy3-labeled secondary antibodies (Jackson) were used. To analyze apoptotic cell numbers, TUNEL (terminal deoxynucleotidyltransferase-mediated dUTP-biotin nick end labeling) analysis was performed according to the manufacturer's instructions (Roche). To detect proliferating cells, mice were sacrificed 90 min after intraperitoneal injection with bromodeoxyuridine (BrdU; 50 μg/g [body weight]). Dissected tissues were treated and sectioned as described above, and BrdU detection was performed according to the manufacturer's instructions (Roche). Cell density and the percentage of BrdU-positive cells were determined on five sections per animal. Statistical significance was tested with the Student *t* test.

Electron microscopy. Achilles tendons of 6-month-old mice were analyzed by electron microscopy as previously described (31). Briefly, tendons were dissected, fixed in 0.1 M sodium cacodylate buffer (pH 7.4) containing 2% glutaraldehyde, rinsed three times in isotonic sodium cacodylate buffer for 30 min, and postfixed in 0.1 M sodium cacodylate (pH 7.4) containing 1% (wt/vol) osmium tetroxide overnight. After dehydration and embedding in Epon 812, samples were cut on a Leica Ultracut S (Deerfield, Ill.) and then stained for 2 h in 5% uranyl acetate and for 7 min in saturated lead citrate solution. Samples were viewed in a Hitachi 7100-B electron microscope (Tokyo, Japan).

Western blot analysis. Rabbit polyclonal anti-Tnmd antibody was raised against a synthetic polypeptide corresponding to amino acids 245 to 252 present in mouse Tnmd (36). Tail tendons from wild type, Tnmd-null, and ChM-I/Tnmd-double-null mice were extracted in homogenizing buffer (8 M urea, 50 mM Tris-HCl [pH 8.0], 1 mM dithiothreitol, 1 mM EDTA). A total of 25 μg of extracted protein were separated on a 15% sodium dodecyl sulfate (SDS)-polyacrylamide gel and transferred to Hybond-P membrane (Amersham). The membranes were preincubated for 4 h at 4°C in blocking buffer and probed with the polyclonal Tnmd, matrilin-2, decorin, collagen α1(III), and collagen α3(VI) antibodies. After an overnight incubation at 4°C, membranes were probed with horseradish peroxidase-conjugated anti-rabbit immunoglobulin G antibody (Amersham). Bound antibodies were visualized by using an enhanced chemiluminescence system (ECL Plus; Amersham). To test the hybridization specificity of the generated Tnmd antibody, it was preincubated for 1 h at room temperature with the polypeptide used for immunization.

OIR. OIR was induced at postnatal day 7 (P7) in wild-type, Tnmd-null, ChM-I-null (11), and Tnmd/ChM-I double-null mice. For 5 days the mice were kept with a lactating female in a ventilation-controlled cage in 75% ± 3% oxygen. Oxygen concentrations were continuously measured (Ahlborn, Holzkirchen, Germany) and automatically adjusted (Almemo 2290; Ahlborn). After five additional days in room air, mice were sacrificed and dissected. One eye was used for retinal whole-mount lectin staining. Eyes were fixed for 2 h in 4% PFA in PBS, retinas were dissected and transferred to 100% methanol at −20°C. After three short washes in PBS and 2 h preincubation in blocking buffer (1% bovine serum albumin, 0.1% Tween 20 in PBS [pH 7.4]), retinas were incubated with fluorescein isothiocyanate-labeled Isolectin B4 (Sigma) in blocking buffer overnight at 4°C. After three washes for 30 min in 1× PBS the retinas were mounted under glass and analyzed by using a confocal microscope (Leica TCS SP2; Leica, Wetzlar, Germany). Vascularized areas were measured and compared at ×2.5 magnification. Each eye was divided in four quadrants and pictures were taken at ×20 magnification to count vessel and branchpoint numbers. The Student *t* test was used for statistical analysis. Three-dimensional reconstruction was performed on representative areas at ×40 magnification by using Imaris software. The second eye was fixed overnight in 4% PFA in PBS (pH 7.4) and then embedded in paraffin. Consecutive 6-μm sections were stained with hematoxylin and eosin, and two independent investigators counted vitreous sprouts in a blind fashion on five stained sections per eye at 50-μm distances.

RESULTS

Generation of mutant mice. Tnmd-deficient mice were generated by interrupting Tnmd expression in exon1 (Fig. 1A). Since Tnmd is located on the X-chromosome, intercrosses of heterozygous targeted mice resulted in hemizygous male and homozygous female mutant mice. Genotyping of 243 newborn offspring derived from heterozygous-hemizygous crosses revealed a normal Mendelian ratio of genotypes. Heterozygous, as well as hemi- and homozygous, mutant mice were viable and had a normal life span. Size and weight measurements did not show differences, and locomotion was normal based on inspection and ink track footprint analysis (data not shown).

Northern blot analysis of thymus, eye, tendon, muscle, and heart tissues from newborn (Fig. 1B) and 1-month-old mutant mice (data not shown) revealed a complete loss of Tnmd mRNA. We raised a peptide antibody against the C-terminal domain of Tnmd and probed extracts from 1-month-old tendon. A single signal was detected in tendon extracts from normal mice, which was not observed in mutant tissue (Fig. 1C) and which was blocked by preincubation of the antibody with the peptide (Fig. 1D). The molecular mass of 16 kDa corresponded to the C-terminal cysteine-rich extracellular domain after cleavage at the putative protease cleavage motif RXXR (4, 12). No signal was observed at 44 kDa, the molecular mass of the uncleaved transmembrane form of Tnmd. These data show that the C-terminal cysteine-rich domain of Tnmd is rapidly cleaved in vivo.

Analysis of tendons. We next analyzed sections from muscle, thymus, heart, liver, spleen, and lung by hematoxylin and eosin staining. No obvious differences were observed between wild-type and Tnmd-deficient mice (data not shown). Whole-skeletal staining of newborn and 6-week-old mice was performed to assess skeletal development, but no size differences, malformations, or signs of contractures were apparent. In addition, X-ray analysis of 6-month-old mice confirmed the absence of skeletal abnormalities (data not shown).

To investigate tendon development and maturation, we prepared histological sections of newborn hind limbs and 1-week-, 2-week-, 1-month-, and 6-month-old Achilles and patellaris tendons. First, we stained them with endomucin, which is a marker of endothelial cells (10). Wild-type tendon and Tnmd-deficient tendons revealed endothelial cells in the peritendineum but not in the proper tendon. No difference was observed in the localization or number of endothelial cells (Fig. 2A).

The size of 1- and 6-month-old Tnmd-deficient Achilles tendons was not altered, but a lower cell density was observed compared to wild-type mice (data not shown). We further assessed cell density in the patellaris and Achilles tendon of newborn, 1-week-old, and 2-week-old mice. A significant reduction of cells ($P < 0.0000015$) was observed in 2-week-old tendons, while cell densities of wild-type and Tnmd-deficient tendons were similar at newborn and P7 stages (Fig. 2B). To test whether the reduction in cell numbers was due to a decreased generation or loss of cells, we investigated apoptotic cell death by TUNEL staining in wild-type and Tnmd-deficient newborn hind limbs and in 1- and 2-week-old patellaris tendons. No difference in the apoptotic index was detectable in any of the analyzed stages (data not shown). We then tested

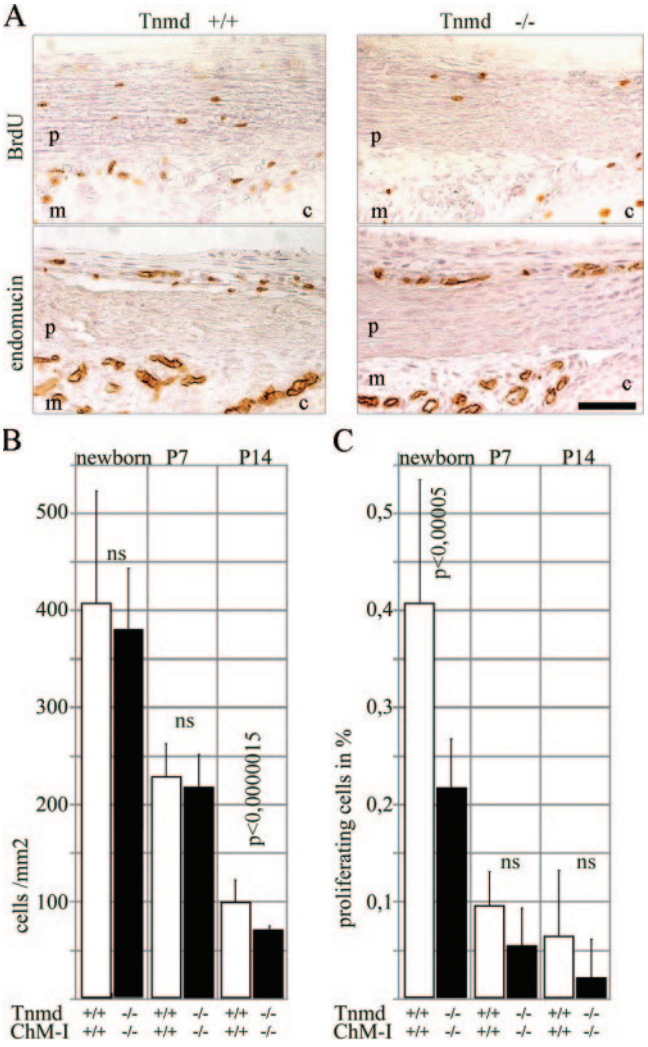

FIG. 2. Proliferation analysis in tendons. (A) BrdU staining of newborn patellaris tendon revealed a decrease of proliferating cells in Tnmd-deficient tendons. Staining with endomucin excluded endothelial origin of the proliferating cells. p, patellaris; m, meniscus; c, cartilage. Bar, 250 μm. (B) Significantly decreased cell densities were found at P14 but not in newborns or at P7. (C) Quantification revealed a significant proliferation deficit in newborns. At P7 and P14 the proliferation of Tnmd-null cells was still reduced compared to the wild type, but the differences were no longer significant (ns).

cell proliferation by BrdU incorporation assays. A decrease of proliferating cells was detected in Achilles, patellaris, and metatarsal tendons of the newborn hind limb. Staining with endomucin, excluded endothelial origin of the proliferating cells (Fig. 2A). Quantification of BrdU-positive cells demonstrated a significant reduction in newborn Tnmd-deficient patellaris tendon ($P < 0.00005$). A proliferation deficit was still present at P7 and P14 but no longer significant (Fig. 2C).

ECM deposition of Tnmd-deficient tenocytes was analyzed in newborn, 1-week-old, and 2-week-old patellaris and Achilles tendons, stages at which remodeling of the tendon collagen network to larger fibril calibers occurs (7, 21). Larger collagen fibrils have less collagen III contribution, which leads to a decrease of collagen III levels during tendon maturation (7,

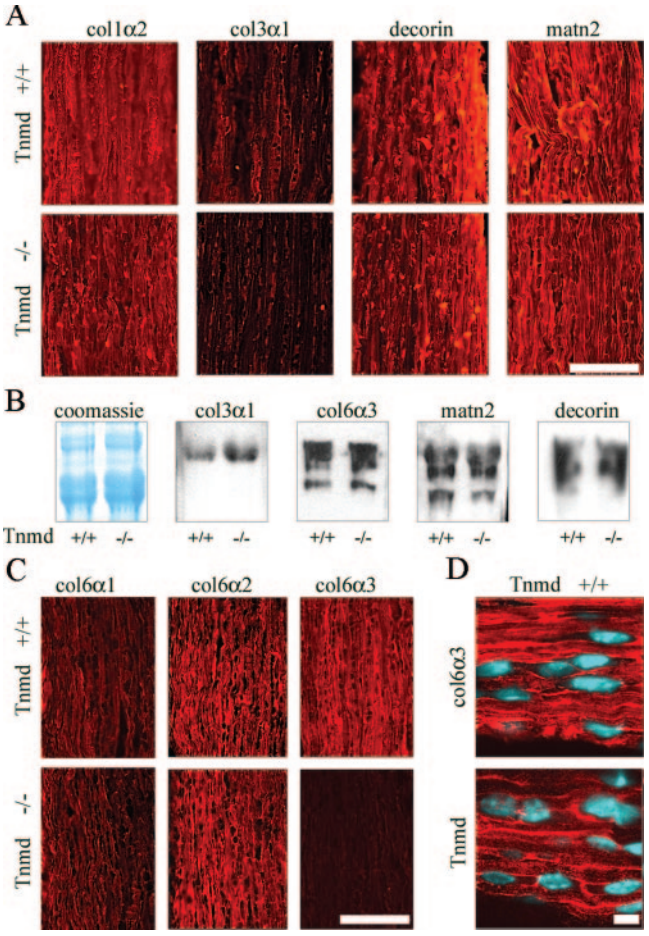

FIG. 3. Analysis of ECM deposition in the tendon. (A) Similar signal intensities were observed by immunostaining for collagen types I (col1α2), matrilin-2 (matn2), and decorin in P14 Achilles tendon. Collagen type III (col3α1) signals were reduced in Tnmd-deficient tendon. Bar, 100 μm. (B) Coomassie blue staining of P14 tail tendon extracts showed similar intensities of the collagen α1(I) band. No differences in signal intensities were found by probing for collagen types III (col3α1, 130 kDa) and VI (col6α3, 180 to 200 kDa), matrilin-2 (matn2, 120 to 150 kDa), and decorin (90 to 120 kDa). (C) Immunostaining for the different α chains of collagen VI revealed similar signal intensities for the collagen VI α1 chain (col6α2) and the α2 chain (col6α2), whereas decreased signal intensity was obtained for the α3 chain (col6α3). Bar, 100 μm. (D) Tnmd and collagen VI α3 showed similar distribution patterns with a predominant pericellular localization. Bar, 10 μm.

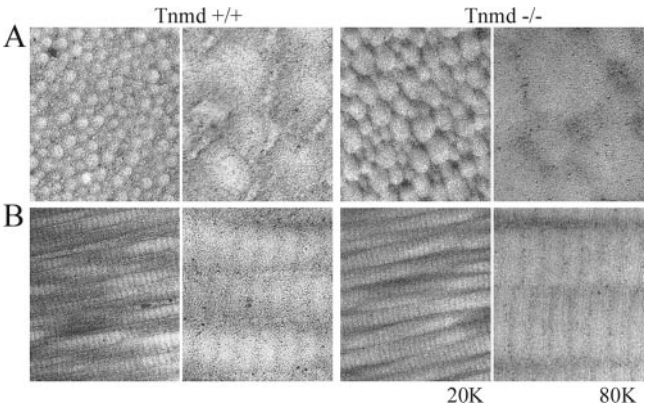

FIG. 4. Ultrastructural analysis of 6-month-old Tnmd-deficient tendons. (A) Cross-sections; (B) longitudinal sections. A shift of the fibril diameter distribution to large diameters was observed. In addition, Tnmd-null tendons showed an uneven and rough surface of the collagen fibrils. Magnifications: ×20,0001 and ×80,000.

22). Immunostaining with an antibody against collagen α2(I) showed an even distribution and equal intensities in wild-type and Tnmd-deficient tendons at all stages investigated (Fig. 3A). Similar levels of collagen I were also observed by Coomassie blue staining of 2-week-old whole tendon extracts (Fig. 3B). Collagen α1(II) was not observed in the tendons of wild-type or Tnmd-deficient mice, indicating that no transdifferentiation to fibrous cartilage occurred (data not shown). Collagen VI is composed of three chains, α1(VI), α2(VI), and α3(VI) (20, 35) and serves as a pericellular anchoring network for tenocytes and collagen fibers (42). Immunofluorescent signals for collagens α1(III) and α3(VI) were consistently weaker in Tnmd-deficient tendons of newborn, 1-week-old, and 2-week-old mice (Fig. 3A and C), although probing extracts from 2-week-old Tnmd-deficient and wild-type tendons showed equal levels (Fig. 3B). Immunofluorescence staining with antibodies to collagens α1(VI) and α2(VI) showed equal signal intensities, confirming that the reduced signal is not caused by lowered collagen VI deposition (Fig. 3C). Since no differences in the deposited amounts were detected, the observed discrepancy in collagens α1(III) and α3(VI) immunostaining signals is likely due to an altered accessibility of these epitopes in Tnmd-deficient mice. Immunostaining for Tnmd showed similar localization of Tnmd and collagen VI in tendons. Both are mainly deposited pericellular, but an additional fibrillar localization was also observed (Fig. 2D). Matrilin-2, which interacts with collagen I (39) and decorin, the major proteoglycan in tendons involved in lateral growth and maturation of tendon fibrils (6, 17), did not show different signal intensities in Tnmd-deficient tendons (Fig. 3A and B). Similarly, immunofluorescent signals for lumican and aggrecan were not affected by the loss of Tnmd expression (data not shown).

Tendon ultrastructure, in particular ECM and collagen fibril morphology, was investigated by electron microscopy. Cross-sections from 6-month-old wild-type Achilles tendon revealed a uniform distribution of collagen fibril diameters typical for the mature stage of tendon maturation (21) (Fig. 4). Cross-sections of Tnmd-null tendons had a greater variation of collagen fibril calibers with a higher proportion of thick fibrils (Fig. 4B). Fibrillar surfaces of Tnmd-null tendons were uneven and rough, whereas collagen fibrils were round and smooth in sections derived from control mice (Fig. 4).

OIR. In vitro studies identified Tnmd as a regulator of endothelial proliferation, but we observed normal vascular densities in Tnmd-deficient tendons. Considering that the lack of phenotype might be due to long-term compensatory changes during development, we decided to analyze experimentally induced neovascularization in mice. OIR provides a reproducible model for retinal neovascularization (46). Exposure of early postnatal mice to high oxygen prevents growth of new retinal vessels and existing vessels are obliterated due to increased apoptosis (1, 49). When the mice are subsequently

exposed to normoxia, the loss of retinal vessels leads to extensive growth of new vessels, which enter the deep layers of the retina and the vitreous.

First, we looked at unchallenged eyes. Since both Tnmd and ChM-I are expressed in the retina and might compensate each other, we analyzed Tnmd-single-null and Tnmd/ChM-I-double-null eyes. Hyaloid vessel regression was not affected; nor was vascularization in the superficial (sl) and the networks of the inner (ipl) and outer plexiform layers (opl) (Fig. 5A and B). We induced OIR at P7 and assessed the retinal vasculature by whole-mount staining with Isolectin-FITC at P17. Retinas of single- and double-mutant eyes had a central obliterated area and dense vascularization in the periphery, similar to wild-type eyes (Fig. 5C and D). Endothelial cells in the superficial, as well as outer and inner plexiform networks, showed no filopodial extensions, and vessel calibers were equal along vessel branches in all layers (Fig. 5E). Quantification of branchpoint numbers in the first-formed superficial layer and the last-formed outer plexiform layers did not reveal any significant changes in retinas lacking both Tnmd and ChM-I (Fig. 5F). Hyaloid vessels were retracted to the lens (data not shown), and retinal endothelial sprouts into the vitreous body were observed at similar frequencies in wild-type and double-null eyes (data not shown).

DISCUSSION

Although posttranslational processing of ChM-I and secretion after cleavage by furin had been experimentally confirmed (3), it was unclear whether Tnmd also is processed in vivo. Homology to ChM-I and a putative protease recognition site indicated cleavage of Tnmd, but probing of eye extracts with an antibody to the C-terminal only detected the membrane-bound form of 44 kDa (36, 37). We raised an antibody to the same Tnmd epitope and identified a fragment of 16 kDa probing tendon extracts. The molecular mass corresponded to a C-terminal fragment of Tnmd after cleavage at the predicted site. In vitro experiments indicated that the cleaved form of the protein inhibits proliferation and tube formation of endothelial cells (36, 37), whereas the uncleaved, membrane-bound Tnmd either increased endothelial proliferation or had no effect at all (37, 40). Here we provide evidence that a cleaved form of Tnmd exists in vivo, which suggests that proteolytic cleavage might be important for Tnmd function in vivo.

To analyze the role of Tnmd in angiogenesis and vasculogenesis, we investigated vessel density by endomucin staining in Tnmd-deficient tendons but did not observe any differences. Compensation by ChM-I is unlikely, since ChM-I is normally not expressed in tendons and also is not upregulated after deletion of Tnmd (data not shown). To challenge the balance of pro- and antiangiogenic factors, we analyzed Tnmd- and ChM-I-deficient mice in a setting in which strong angiogenesis is suddenly induced. However, OIR induced in mice lacking both Tnmd and ChM-I did not lead to altered retinal neovascularization. Thus, we could not find any evidence for an involvement of ChM-I or Tnmd in the regulation of angiogenesis or retinal neovascularization in vivo.

Tnmd-deficient mice displayed a severe decrease in proliferating cells in newborn tendons. This postnatal proliferation deficit probably caused reduced cell density in P14 and adult

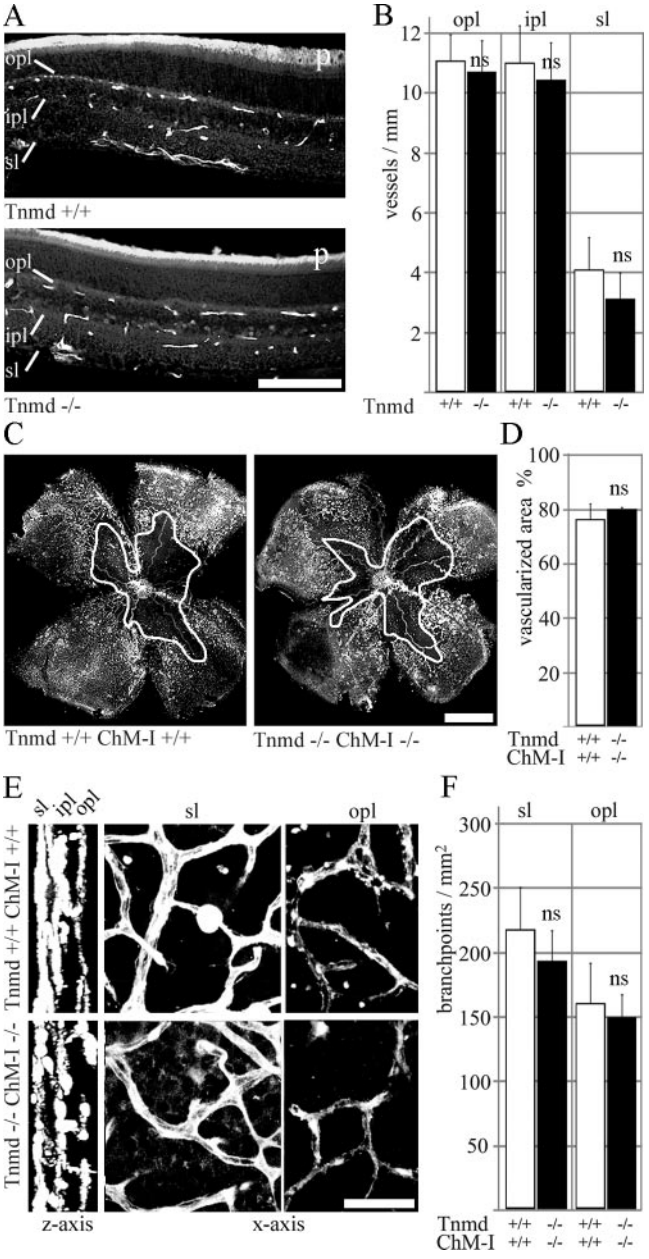

FIG. 5. Analysis of retinal neovascularization. (A) Endomucin staining of 1-month-old retinas. Superficial (sl), inner-plexiform (ipl), and outer plexiform (opl) vessel networks were completely formed in Tnmd-deficient retinas. (B) All layers had similar vessel numbers compared to wild-type eyes. p, photoreceptors. Bar, 100 μm. (C) Whole-mount lectin-staining failed to detect differences in the vascularized area of wild-type and double-null retinas after OIR at P7. The white outline indicates unvascularized area. Bar, 1 mm. (D) Quantification of the neovascular area/whole retina showed equal percentages for wild-type and double-null eyes. (E) After three-dimensional reconstruction, the three vascular layers were clearly distinguishable (z axis). Wild-type and double-null retinas displayed similar vascular morphology in the superficial (sl) and the outer plexiform vascular networks (opl). (F) Quantification of branchpoints in the superficial and outer plexiform layers did not reveal significant differences between wild-type and double-null eyes. ns, not significant. Bar, 20 μm.

tendons, since no apoptotic loss of cells was observed. Interestingly, the C-terminal domain of ChM-I induced proliferation of chondrocytes in vitro (27), but mice lacking ChM-I had no alterations in skeletal development or chondrocyte proliferation (11, 32). Despite the lower cell numbers, Tnmd-deficient tendons had the same size as wild-type tendons, suggesting that either the remaining tenocytes were able to compensate the loss of cells or that the turnover of ECM is delayed in Tnmd-deficient tendons.

The deposited amounts of collagen types I, α1(III), and α3(VI) were similar in wild-type and Tnmd-deficient tendons. However, weaker signals were found by immunostaining for collagen α1(III) and collagen α3(VI). The reduction of collagen α3(VI) signals was further investigated by applying collagen α1(VI) and α2(VI) antibodies, which showed equal signal intensities from wild-type and Tnmd-deficient tendons. The reduced accessibility of collagen α1(III) and α3(VI) epitopes in Tnmd-deficient tendons might indicate structural changes in Tnmd-deficient tendons. Although collagen III is associated with the collagen fibrils, collagen VI is concentrated in the pericellular space, where Tnmd protein can also be found. Collagen VI is bound directly by tenocyte cell surface receptors, and its interaction with a complex of proteoglycans and matrilins was suggested to be important for the regulation of growing collagen I fibrils (33, 42, 48). Tnmd-null tendons showed a greater variation of collagen fibril diameters and an increase of the maximal fibril diameters, but we did not observe altered amounts of proteoglycans. Therefore, we speculate that lack of Tnmd leads to changes in the pericellular collagen VI network, indicated by the altered accessibility of collagen α3(VI) epitopes. This might lead to inefficient presentation of collagen fibril regulating factors as proteoglycans and finally result in the observed altered tendon ultrastructure.

An increase of large-diameter fibrils in tendon and irregular contacts between tenocytes and fibrils were described in mice lacking thrombospondin-2 (thbs2), an extracellular modular glycoprotein, which also has angiogenesis regulating properties (8, 9, 29). thbs2 interacts with a number of cell surface receptors, including integrin αvβ3 (14, 15), which is present on endothelial cells and tenocytes (16, 24, 25). The C-terminal cysteine-rich domain of Tnmd was recently shown to specifically inhibit endothelial adhesion to vitronectin (37), which, taken together with the similar phenotypes of Tnmd- and thbs2-deficient mice, suggest that changes in cell matrix interaction might cause the proliferation deficit and collagen fibril enlargement of Tnmd-deficient tendons.

ACKNOWLEDGMENTS

We thank Edward Fellows for reading the manuscript, Attila Aszódi for helpful suggestions, and Nikola Popov for supervision and administrative support at the University of Plovdiv, Plovdiv, Bulgaria. We are indebted to Rupert Timpl, Takako Sasaki, Richard Holmdahl, Åke Oldberg, Dietmar Vestweber, and Raimund Wagener for providing antibodies.

R.F. is supported by the Fonds der Chemischen Industrie and the Max Planck Society.

REFERENCES

1. **Alon, T., I. Hemo, A. Itin, J. Pe'er, J. Stone, and E. Keshet.** 1995. Vascular endothelial growth factor acts as a survival factor for newly formed retinal vessels and has implications for retinopathy of prematurity. Nat. Med. **1:**1024–1028.
2. **Aszódi, A., J. F. Bateman, E. Hirsch, M. Baranyi, E. B. Hunziker, N. Hauser, Z. Bösze, and R. Fässler.** 1999. Normal skeletal development of mice lacking matrilin-1: redundant function of matrilins in cartilage? Mol. Cell. Biol. **19:**7841–7845.
3. **Azizan, A., N. Holaday, and P. J. Neame.** 2001. Post-translational processing of bovine chondromodulin-I. J. Biol. Chem. **276:**23632–23638.
4. **Barr, P. J.** 1991. Mammalian subtilisins: the long-sought dibasic processing endoproteases. Cell **66:**1–3.
5. **Benjamin, M., and J. R. Ralphs.** 2000. The cell and developmental biology of tendons and ligaments. Int. Rev. Cytol. **196:**85–130.
6. **Birk, D. E., M. V. Nurminskaya, and E. I. Zycband.** 1995. Collagen fibrillogenesis in situ: fibril segments undergo post-depositional modifications resulting in linear and lateral growth during matrix development. Dev. Dyn. **202:**229–243.
7. **Birk, D. E., and R. Mayne.** 1997. Localization of collagen types I, III, and V during tendon development. Changes in collagen types I and III are correlated with changes in fibril diameter. Eur. J. Cell Biol. **72:**352–361.
8. **Bornstein, P., L. C. Armstrong, K. D. Hankenson, T. R. Kyriakides, and Z. Yang.** 2000. Thrombospondin 2, a matricellular protein with diverse functions. Matrix Biol. **19:**557–568.
9. **Bornstein, P., A. Agah, and T. R. Kyriakides.** 2004. The role of thrombospondins 1 and 2 in the regulation of cell-matrix interactions, collagen fibril formation, and the response to injury. Int. J. Biochem. Cell. Biol. **36:**1115–1125.
10. **Brachtendorf, G., A. Kuhn, U. Samulowitz, R. Knorr, E. Gustafsson, A. J. Potocnik, R. Fässler, and D. Vestweber.** 2001. Early expression of endomucin on endothelium of the mouse embryo and on putative hematopoietic clusters in the dorsal aorta. Dev. Dyn. **222:**410–419.
11. **Brandau, O., A. Aszódi, E. B. Hunziker, P. J. Neame, D. Vestweber, and R. Fässler.** 2002. Chondromodulin I is dispensable during enchondral ossification and eye development. Mol. Cell. Biol. **22:**6627–6635.
12. **Brandau, O., A. Meindl, R. Fässler, and A. Aszódi.** 2001. A novel gene, tendin, is strongly expressed in tendons and ligaments and shows high homology with chondromodulin-I. Dev. Dyn. **221:**72–80.
13. **Chakravarti, S., T. Magnuson, J. H. Lass, K. J. Jepsen, C. LaMantia, and H. Carroll.** 1998. Lumican regulates collagen fibril assembly: skin fragility and corneal opacity in the absence of lumican. J. Cell Biol. **141:**1277–1286.
14. **Chen, H., D. K. Strickland, and D. F. Mosher.** 1996. Metabolism of thrombospondin 2: binding and degradation by 3T3 cells and glycosaminoglycan-variant Chinese hamster ovary cells. J. Biol. Chem. **271:**15993–15999.
15. **Chen, H., J. Sottile, K.M. O'Rourke, V. M. Dixit, and D. F. Mosher.** 1994. Properties of recombinant mouse thrombospondin 2 expressed in *Spodoptera* cells. J. Biol. Chem. **269:**32226–32232.
16. **Cheresh, D. A.** 1987. Human endothelial cells synthesize and express an Arg-Gly-Asp-directed adhesion receptor involved in attachment to fibrinogen and von Willebrand factor. Proc. Natl. Acad. Sci. USA **84:**6471–6475.
17. **Corsi, A., T. Xu, X. D. Chen, A. Boyde, J. Liang, M. Mankani, B. Sommer, R. V. Iozzo, I. Eichstetter, P. G. Robey, P. Bianco, and M. F. Young.** 2002. Phenotypic effects of biglycan deficiency are linked to collagen fibril abnormalities, are synergized by decorin deficiency, and mimic Ehlers-Danlos-like changes in bone and other connective tissues. J. Bone Miner. Res. **17:**1180–1189.
18. **Danielson, K. G., H. Baribault, D. F. Holmes, H. Graham, K. E. Kadler, and R. V. Iozzo.** 1997. Targeted disruption of decorin leads to abnormal collagen fibril morphology and skin fragility. J. Cell Biol. **136:**729–743.
19. **Dziadek, M., P. Darling, R. Z. Zhang, T. C. Pan, E. Tillet, R. Timpl, and M. L. Chu.** 1995. Expression of collagen α1(VI), α2(VI), and α3(VI) chains in the pregnant mouse uterus. Biol. Reprod. **52:**885–894.
20. **Engvall, E., H. Hessle, and G. Klier.** 1986. Molecular assembly, secretion, and matrix deposition of type VI collagen. J. Cell Biol. **102:**703–710.
21. **Ezura, Y., S. Chakravarti, Å. Oldberg, I. Chervoneva, and D. E. Birk.** 2000. Differential expression of lumican and fibromodulin regulate collagen fibrillogenesis in developing mouse tendons. J. Cell Biol. **151:**779–788.
22. **Fleischmajer, R., J. S. Perlish, R. E. Burgeson, F. Shaikh-Bahai, and R. Timpl.** 1990. Type I and type III collagen interactions during fibrillogenesis. Ann. N. Y. Acad. Sci. **580:**161–175.
23. **Funaki, H., S. Sawaguchi, K. Yaoeda, Y. Koyama, E. Yaoita, S. Funaki, M. Shirakashi, Y. Oshima, C. Shukunami, Y. Hiraki, H. Abe, and T. Yamamoto.** 2001. Expression and localization of angiogenic inhibitory factor, chondromodulin-I, in adult rat eye. Investig. Ophthalmol. Vis. Sci. **42:**1193–1200.
24. **Harwood, F. L., A. Z. Monosov, R. S. Goomer, R. H. Gelberman, S. C. Winters, M. J. Silva, and D. Amiel.** 1998. Integrin expression is upregulated during early healing in a canine intrasynovial flexor tendon repair and controlled passive motion model. Connect. Tissue Res. **39:**309–316.
25. **Harwood, F. L., R. S. Goomer, R. H. Gelberman, M. J. Silva, and D. Amiel.** 1999. Regulation of αvβ3 and α5β1 integrin receptors by basic fibroblast growth factor and platelet-derived growth factor-BB in intrasynovial flexor tendon cells. Wound Repair Regen. **7:**381–388.
26. **Hiraki, Y., H. Tanaka, H. Inoue, J. Kondo, A. Kamizono, and F. Suzuki.** 1991. Molecular cloning of a new class of cartilage-specific matrix, chondromodulin-I, which stimulates growth of cultured chondrocytes. Biochem. Biophys. Res. Commun. **175:**971–977.

27. **Inoue, H., J. Kondo, T. Koike, C. Shukunami, and Y. Hiraki.** 1997. Identification of an autocrine chondrocyte colony-stimulating factor: chondromodulin-I stimulates the colony formation of growth plate chondrocytes in agarose culture. Biochem. Biophys. Res. Commun. **241:**395–400.
28. **Kjaer, M.** 2004. Role of extracellular matrix in adaptation of tendon and skeletal muscle to mechanical loading. Physiol. Rev. **84:**649–698.
29. **Kyriakides, T. R., Y. H. Zhu, L. T. Smith, S. D. Bain, Z. Yang, M. T. Lin, K. G. Danielson, R. V. Iozzo, M. LaMarca, C. E. McKinney, E. I. Ginns, and P. Bornstein.** 1998. Mice that lack thrombospondin 2 display connective tissue abnormalities that are associated with disordered collagen fibrillogenesis, an increased vascular density, and a bleeding diathesis. J. Cell Biol. **140:**419–430.
30. **McNeilly, C. M., A. J. Banes, M. Benjamin, and J. R. Ralphs.** 1996. Tendon cells in vivo form a three dimensional network of cell processes linked by gap junctions. J. Anat. **189:**593–600.
31. **Mikic, B., B. J. Schalet, R. T. Clark, V. Gaschen, and E. B. Hunziker.** 2001. GDF-5 deficiency in mice alters the ultrastructure, mechanical properties and composition of the Achilles tendon. J. Orthop. Res. **19:**365–371.
32. **Nakamichi, Y., C. Shukunami, T. Yamada, K. Aihara, H. Kawano, T. Sato, Y. Nishizaki, Y. Yamamoto, M. Shindo, K. Yoshimura, T. Nakamura, N. Takahashi, H. Kawaguchi, Y. Hiraki, and S. Kato.** 2003. Chondromodulin I is a bone remodeling factor. Mol. Cell. Biol. **23:**636–644.
33. **Nareyeck, G., D. G. Seidler, D. Troyer, J. Rauterberg, H. Kresse, and E. Schonherr.** 2004. Differential interactions of decorin and decorin mutants with type I and type VI collagens. Eur. J. Biochem. **271:**3389–3398.
34. **Neame, P. J., J. T. Treep, and C. N. Young.** 1990. An 18-kDa glycoprotein from bovine nasal cartilage. Isolation and primary structure of small, cartilage-derived glycoprotein. J. Biol. Chem. **265:**9628–9633.
35. **Odermatt, E., J. Risteli, V. van Delden, and R. Timpl.** 1983. Structural diversity and domain composition of a unique collagenous fragment (intima collagen) obtained from human placenta. Biochem. J. **211:**295–302.
36. **Oshima, Y., C. Shukunami, J. Honda, K. Nishida, F. Tashiro, J. Miyazaki, Y. Hiraki, and Y. Tano.** 2003. Expression and localization of tenomodulin, a transmembrane type chondromodulin-I-related angiogenesis inhibitor, in mouse eyes. Investig. Ophthalmol. Vis. Sci. **44:**1814–1823.
37. **Oshima, Y., K. Sato, F. Tashiro, J. Miyazaki, K. Nishida, Y. Hiraki, Y. Tano, and C. Shukunami.** 2004. Anti-angiogenic action of the C-terminal domain of tenomodulin that shares homology with chondromodulin-I. J. Cell Sci. **117:**2731–2744.
38. **Osoegawa, K., M. Tateno, P. Y. Woon, E. Frengen, A. G. Mammoser, J. J. Catanese, Y. Hayashizaki, and P. J. de Jong.** 2000. Bacterial artificial chromosome libraries for mouse sequencing and functional analysis. Genome Res. **10:**116–128.
39. **Piecha, D., C. Wiberg, M. Mörgelin, D. P. Reinhardt, F. Deak, P. Maurer, and M. Paulsson.** 2002. Matrilin-2 interacts with itself and with other extracellular matrix proteins. Biochem. J. **367:**715–721.
40. **Pisani, D. F., P. M. Pierson, A. Massoudi, L. Leclerc, A. Chopard, J. F. Marini, and C. A. Dechesne.** 2004. Myodulin is a novel potential angiogenic factor in skeletal muscle. Exp. Cell Res. **292:**40–50.
41. **Ralphs, J. R., A. D. Waggett, and M. Benjamin.** 2002. Actin stress fibres and cell-cell adhesion molecules in tendons: organisation in vivo and response to mechanical loading of tendon cells in vitro. Matrix Biol. **21:**67–74.
42. **Ritty, T. M., R. Roth, and J. E. Heuser.** 2003. Tendon cell array isolation reveals a previously unknown fibrillin-2-containing macromolecular assembly. Structure **11:**1179–1188.
43. **Sánchez-Pulido, L., D. Devos, and A. Valencia.** 2002. BRICHOS: a conserved domain in proteins associated with dementia, respiratory distress and cancer. Trends Biochem. Sci. **27:**329–332.
44. **Scott, J. E., C. R. Orford, and E. W. Hughes.** 1981. Proteoglycan-collagen arrangements in developing rat tail tendon: an electron microscopic and biochemical investigation. Biochem. J. **195:**573–581.
45. **Shukunami, C., Y. Oshima, and Y. Hiraki.** 2001. Molecular cloning of *tenomodulin*, a novel *chondromodulin-I* related gene. Biochem. Biophys. Res. Commun. **280:**1323–1327.
46. **Smith, L. E., E. Wesolowski, A. McLellan, S. K. Kostyk, R. D'Amato, R. Sullivan, and P. A. D'Amore.** 1994. Oxygen-induced retinopathy in the mouse. Investig. Ophthalmol. Vis. Sci. **35:**101–111.
47. **Svensson, L., A. Aszódi, F. P. Reinholt, R. Fässler, D. Heineg(angst)ard, and Å. Oldberg.** 1999. Fibromodulin-null mice have abnormal collagen fibrils, tissue organization, and altered lumican deposition in tendon. J. Biol. Chem. **274:**9636–9647.
48. **Wiberg, C., A. R. Klatt, R. Wagener, M. Paulsson, J. F. Bateman, D. Heinegård, and M. Mörgelin.** 2003. Complexes of matrilin-1 and biglycan or decorin connect collagen VI microfibrils to both collagen II and aggrecan. J. Biol. Chem. **278:**37698–37704.
49. **Yamada, H., E. Yamada, S. Hackett, H. Ozaki, N. Okamoto, and P. Campochiaro.** 1999. Hyperoxia causes decreased expression of vascular endothelial growth factor and endothelial cell apoptosis in adult retina. J. Cell Physiol. **179:**149–156.
50. **Yamana, K., H. Wada, Y. Takahashi, H. Sato, Y. Kasahara, and M. Kiyoki.** 2001. Molecular cloning and characterization of CHM1L, a novel membrane molecule similar to chondromodulin-I. Biochem. Biophys. Res. Commun. **280:**1101–1106.